Aerodynamic Loading of an Axial Compressor Stator: Effect of Blade Number Reduction

Gabriel Virto Chirhuana, Selim Aktas

Technical University of Munich, Chair of Turbomachinery and Flight Propulsion

CFD - Design of Turbomachinery

Abstract

An axial single-stage compressor is investigated using Computational Fluid Dynamics to quantify the aerodynamic consequences of stator blade number reduction. Two configurations are compared: a reference design with 44 stator blades and a modified design with 38 blades. While the overall stage total pressure ratio remains largely unaffected due to unchanged rotor operation, distinct differences arise in stator loss generation and flow stability. The reduced-solidity configuration exhibits lower losses at high mass flow rates but a pronounced deterioration in performance near the surge limit, associated with enhanced adverse pressure gradients, boundary layer thickening, and flow separation. The analysis combines 1D performance maps with 2D radial distributions and 3D flow visualizations to establish a consistent physical interpretation of the observed trends.

Nomenclature

CFD Computational Fluid Dynamics

ADP Aerodynamic Design Position

CC Choking Condition

SC Surge Condition

ω Total pressure loss coefficient [-]

p Pressure [Pa]

p_t Total pressure [Pa]

Subscripts:

1 Inlet (before Rotor)

2 Between Rotor/Stator

3 Outlet (after Stator)

R Rotor

S Stator

Introduction

Axial compressors are critical components in modern gas turbines, where aerodynamic efficiency must be balanced against structural and economic constraints [1]. In this context, reducing the number of stator blades represents an attractive design modification, offering decreased weight, reduced manufacturing complexity, and lower wetted surface area. However, such a reduction inherently decreases cascade solidity and increases blade loading, potentially compromising aerodynamic stability.

The present work investigates this trade-off by comparing a reference stator with 44 blades to a reduced-solidity configuration with 38 blades. The analysis focuses on stator aerodynamics, with particular emphasis on loss generation, flow turning capability, and stability limits across the compressor operating range.

Problem Description

The objective of this study is to quantify the aerodynamic impact of stator blade number reduction while maintaining identical rotor geometry and operating conditions. Any observed differences can therefore be attributed exclusively to modifications in the stator flow field.

1. Background and Motivation

The stator in an axial compressor removes swirl from the rotor exit flow and converts kinetic energy into static pressure through diffusion. Its aerodynamic performance is governed by the cascade solidity, defined as $\sigma = s/t$, where s is the chord length and t the blade pitch. Reducing the blade count increases t, thereby decreasing solidity and reducing the level of geometric flow guidance [1].

A decrease in solidity requires each blade to sustain higher aerodynamic loading to achieve equivalent flow turning. This results in steeper adverse pressure gradients along the suction surface, increasing susceptibility to boundary layer separation, particularly under off-design conditions approaching surge. While the rotor continues to define the work input and stage pressure rise, the stator becomes the limiting component in terms of loss generation and flow stability.

Three operating points are considered: choking condition (CC), aerodynamic design point (ADP) and surge condition (SC). These points enable a systematic assessment of the trade-off between efficiency and stability margin.

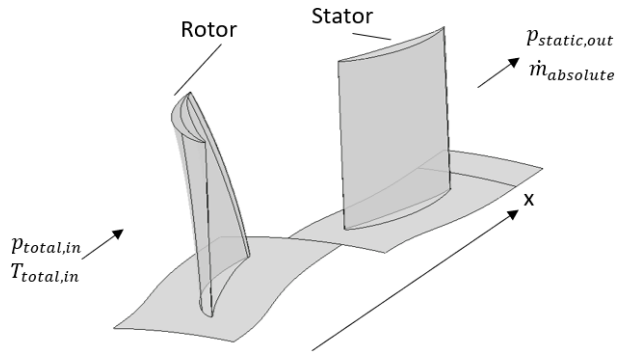

Figure 1: Computational domain and applied boundary conditions

2. Assumptions

The reduction in stator blade number primarily affects the aerodynamic behavior through a decrease in cascade solidity. This modification is expected to influence:

- Flow turning capability due to reduced geometric guidance
- Diffusion strength within the stator passage
- Loss generation associated with boundary layer development and secondary flows

A lower surface area reduces viscous losses under high mass flow conditions, particularly near choking. However, the increased blade pitch requires each blade to sustain higher aerodynamic loading to achieve the same level of swirl removal and pressure recovery.

This elevated loading intensifies adverse pressure gradients along the suction surface, promoting boundary layer thickening, flow deviation, and potential separation, especially as the operating point approaches the surge limit. Consequently, while the modification offers structural and efficiency-related benefits, it is expected to reduce aerodynamic robustness and stability margin under off-design conditions.

3. Compressor model and Numerical Setup

The objective of this project is to evaluate the aerodynamic loading and stage performance resulting from a reduction in stator blade count to 38. The rotor geometry and rotational speed remain unchanged in order to isolate the aerodynamic effects exclusively to the stator flow field. This geometric modification inherently requires the remaining blades to achieve the necessary flow diffusion and swirl removal over a larger passage area [1].

To ensure computational efficiency, a single-passage model with periodic boundary conditions is employed, assuming rotationally symmetric flow through the compressor stage. The computational grid is generated using Ansys TurboGrid, applying a structured hexahedral mesh with a target passage size of approximately 120,000 nodes.

Boundary conditions and convergence criteria are defined in CFX Pre, with the corre-

sponding model parameters summarized in Table 1. The steady-state, three-dimensional Reynolds-Averaged Navier–Stokes (RANS) equations are solved using the k-ϵ turbulence model to capture turbulent mixing and dissipation. The working fluid is modeled as an ideal gas. All simulations are performed using Ansys CFX 2025 R1.

Meshing Parameter	**Value**
Node count Rotor (Proj)	149 295
Node count Stator (Proj)	145 350
Mesh Type	H-grid
y^+	50
Rotor gap	2 %
Stator gap	no gap

Boundary Conditions	**Value**
Inlet total pressure	101 325 Pa
Inlet total temperature	293.15 K
Outlet back pressure	85 to 108.5 kPa
Turbulence model	k-ϵ
Heat Transfer	Total Energy
Max. error	10^{-6}
Max. iterations	100

Table 1: CFD Model and Boundary Conditions

Results / Evaluation

The simulated configurations are evaluated using CFX Post-Processing. First, the operating characteristics of both configurations are compared across varying back pressures using a 1D performance map. Based on this analysis, three representative operating points are selected and examined in detail through 2D radial profiles and 3D flow field visualizations.

1. Comparison in the Performance Map 1D

1.1 Total Pressure Ratio

The primary objective of a compressor stage is to achieve a high total pressure rise. This consists of a pressure increase across the rotor and a pressure drop across the stator due to loss-generating processes. The total pressure ratios are defined as:

$$\Pi_{t,Stage} = \frac{p_{t3}}{p_{t1}} \quad \Pi_{t,S} = \frac{p_{t3}}{p_{t2}} \tag{1}$$

Figure 2 presents the total pressure ratios for both the stage and the stator. The stage and the rotor exhibit nearly identical pressure ratio characteristics for both configurations. This indicates that the stator modification does not induce any significant upstream influence on the rotor. Therefore, the following discussion focuses on the stator behavior.

This behavior is physically consistent with turbomachinery fundamentals: the rotor provides the primary energy input to the flow, while the stator primarily performs diffusion

and static pressure recovery. As a result, the unchanged rotor operation leads to an essentially constant stage pressure ratio.

At the stator level, a slightly higher total pressure ratio is observed under choking conditions. The increased blade spacing accommodates higher mass flow rates more effectively, reducing blockage effects. Consequently, the reduction in blade number does not compromise the stage's compression capability from a thermodynamic standpoint. However, preserving the pressure ratio alone does not ensure favorable aerodynamic performance, as becomes evident when considering loss generation and flow behavior.

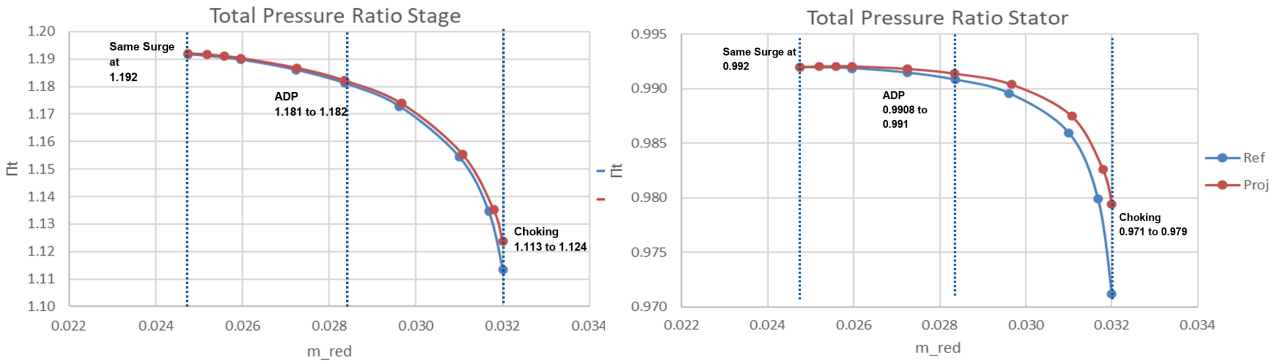

Figure 2: Total Pressure Ratio Stage and Stator

1.2 Total Pressure Loss Coefficient

For the evaluation of pressure losses, the total pressure loss coefficient of the stator is defined as:

$$\omega = \frac{p_{t2} - p_{t3}}{p_{t2} - p_2} \tag{2}$$

The 38-blade configuration exhibits lower losses at choking and at ADP, but higher losses as the operating point approaches surge. The reduction in blade count decreases the wetted surface area, thereby reducing profile and friction losses. This results in a slight efficiency improvement under high mass flow and near-design conditions.

In contrast, near surge, the reduced blade count increases the aerodynamic loading per blade. This leads to stronger adverse pressure gradients within the stator passage, promoting boundary layer thickening, flow separation, and enhanced secondary flow losses. As a result, the stator's ability to efficiently diffuse the flow deteriorates under high back pressure, leading to a significant increase in losses.

Overall, the modified stator improves performance at high mass flow rates but penalizes operation near the stability limit.This behavior represents the classical trade-off between aerodynamic efficiency and stability margin in reduced solidity compressor designs.

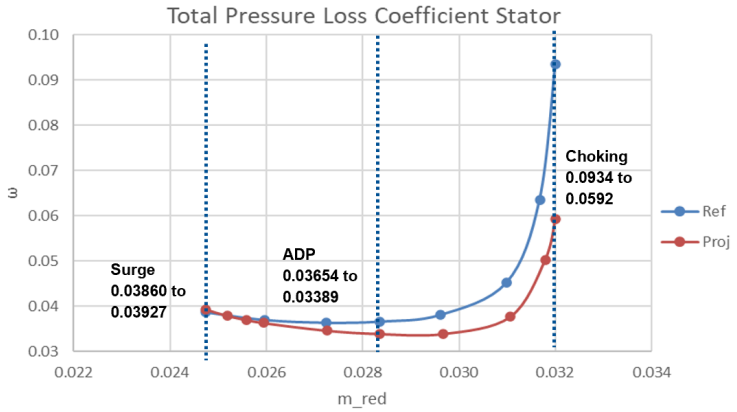

Figure 3: Total Pressure Loss Coefficient in the stator

1.3 Diffusion Number

The diffusion number is consistently higher for the 38-blade configuration, indicating stronger flow deceleration within the stator passages. This increase is caused by the reduced blade count, which leads to a larger pitch and lower solidity. As a result, the same flow turning must be achieved with fewer blades, increasing the aerodynamic loading on each blade and intensifying the diffusion process. Consequently, stronger adverse pressure gradients develop, reducing boundary layer stability and increasing the risk of flow separation. This effect becomes particularly critical near surge, where the flow is highly sensitive to pressure recovery and prone to separation.

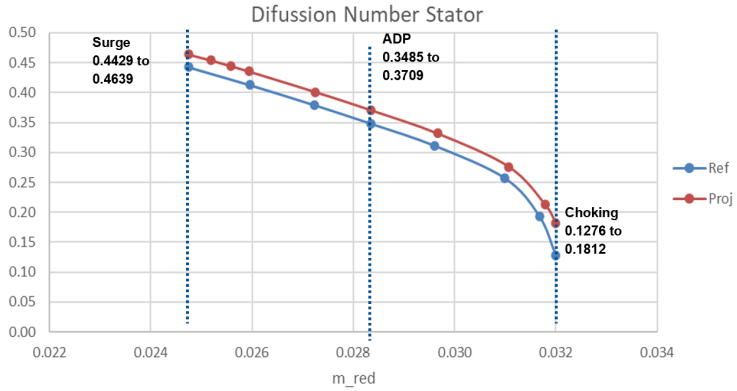

Figure 4: Diffusion number in the Stator

1.4 Flow Turning

The stator turning behavior varies significantly with operating condition, showing slightly increased turning at choking and reduced turning at ADP and near surge.

At choking, the high mass flow results in strong flow momentum, while the increased blade pitch reduces blockage. Under these conditions, the flow remains attached and follows

the blade geometry, allowing effective or slightly improved turning. In contrast, at ADP and near surge, increasing back pressure leads to stronger adverse pressure gradients. Combined with higher blade loading, this reduces the ability of the flow to follow the blade curvature. Boundary layer growth and flow deviation increase, resulting in a loss of turning capability.

Overall, the reduced solidity configuration exhibits diminished flow turning contributing to performance degradation near surge.

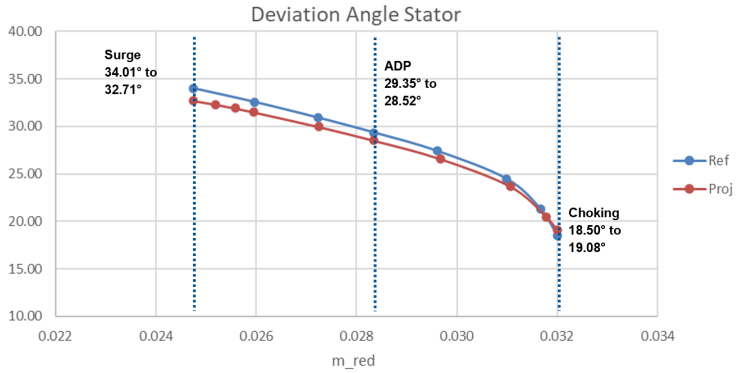

Figure 5: Deviation angle in the Stator

1.5 Exit flow angle

The stator exit angle α_3 is consistently lower in the 38-blade configuration at ADP and near surge. The reduced solidity leads to diminished aerodynamic control over the flow, resulting in increased deviation as the flow leaves the blade at a larger angle relative to the camber line. This reduces the effective turning angle within the stator. Consequently, the lower exit angle indicates incomplete swirl removal and the presence of residual kinetic energy in the flow.

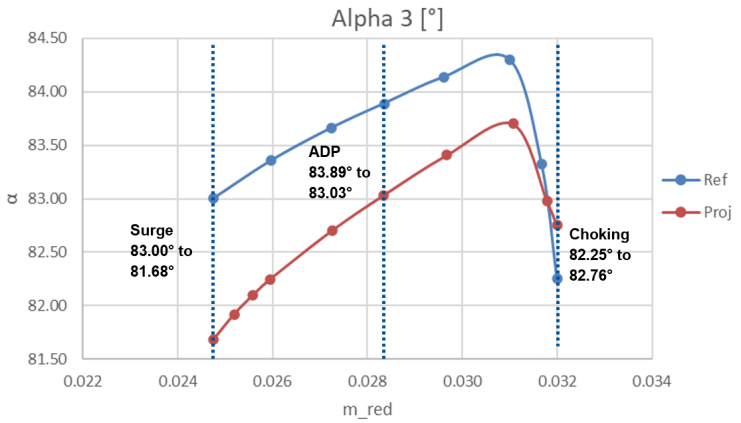

Figure 6: Exit flow angle in the stator

2. Comparison of radial profiles 2D

2.1 Flow Angles at the Stator Inlet

The flow angles at the stator inlet, represented by the absolute flow angle α_2 and the relative flow angle β_2, provide insight into the rotor–stator interaction and the swirl level at the rotor exit.

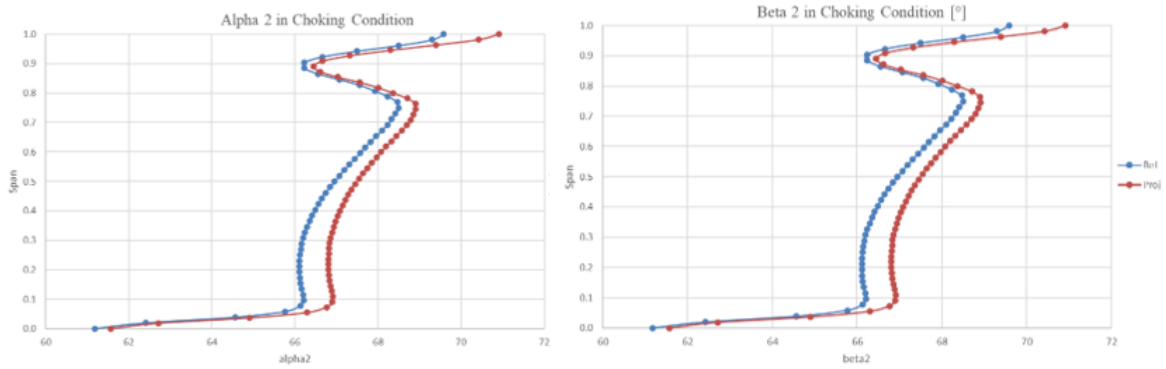

Figure 7: Flow angles at the stator inlet at choking Condition

At CC, as shown in Figure 7, the modified configuration exhibits slightly higher values of α_2 and β_2 across most of the span. This indicates a more axial flow direction and reduced swirl. The enlarged stator passage accommodates the high mass flow more effectively, resulting in lower blockage and reduced blade–flow interaction.

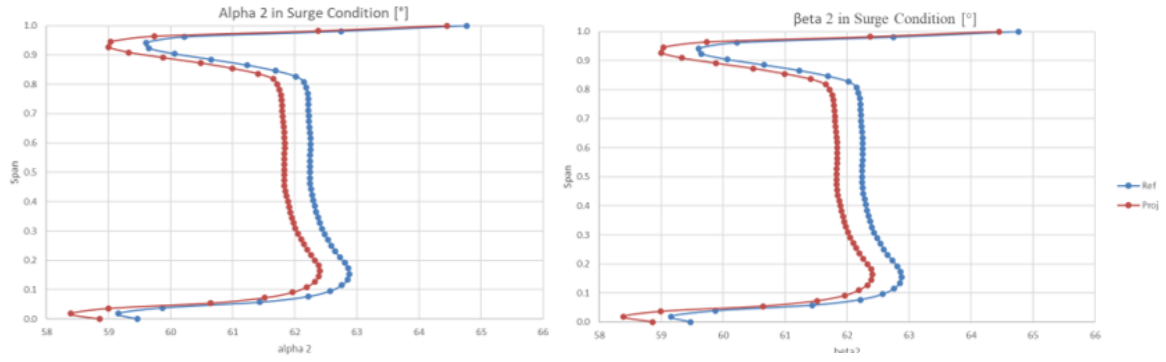

Figure 8: Flow angles at the stator inlet at surge condition

At near surge; as shown in Figure 8, the trend reverses, with the modified configuration exhibiting lower inlet flow angles. This indicates a reduction in swirl removal capability. As the back pressure increases, the flow becomes more sensitive to adverse pressure gradients. The reduced stator solidity weakens the aerodynamic guidance of the flow, leading to increased deviation and consequently lower effective inlet angles.

As a result, the stator loses its ability to properly control the incoming swirl from the rotor under these conditions.

2.2 Pressure Coefficient

The pressure coefficient C_p distribution describes the blade surface loading and is directly related to aerodynamic forces, diffusion, and flow stability. The rotor C_p distribution remains almost unchanged across all operating conditions, confirming that the rotor performance is not affected by the stator modification.

For the stator at choking condition, the pressure distribution is more uniform in the modified configuration, and no pronounced suction peak is observed. The loading is redistributed along the chord, indicating a milder pressure gradient.

At ADP and near surge, the modified stator exhibits a larger pressure difference between the suction and pressure sides, indicating increased aerodynamic loading. This pressure difference becomes more pronounced as the operating point approaches surge, and the stator approaches critical loading conditions. This behavior is a direct consequence of the increased blade pitch, reduced solidity, and higher loading per blade.

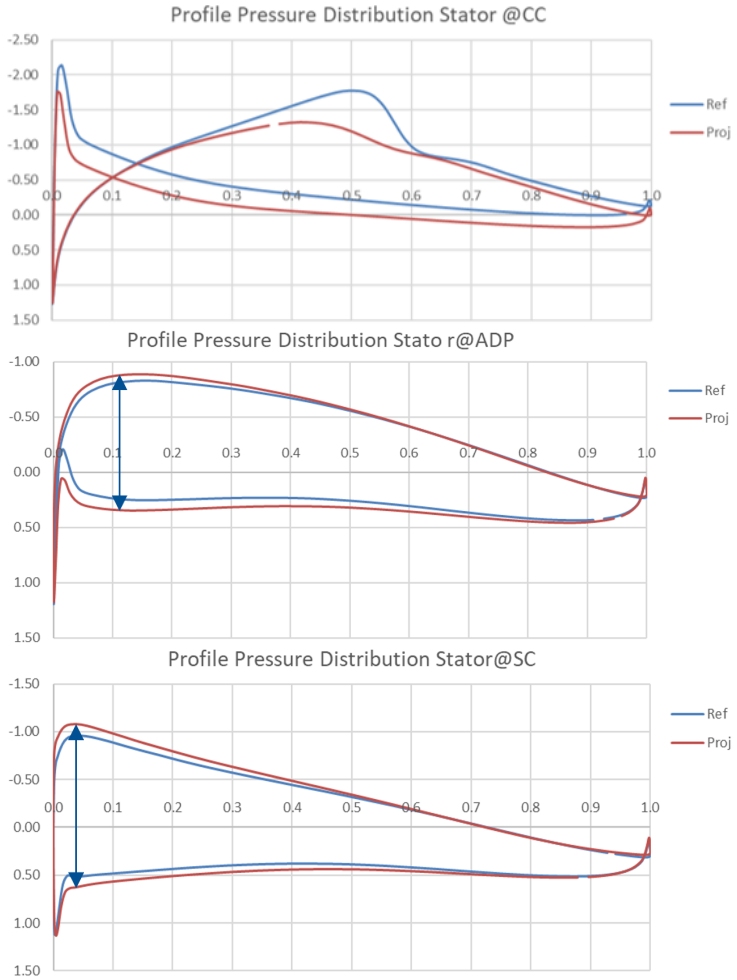

Figure 9: Pressure coefficient distribution showing a clear loading penalty at ADP and Surge Condition

3. Comparison in 3D flow field

3.1 Separation at Stator

Figure 10 illustrates separation phenomena within the stator passages, with the most pronounced differences occurring under choking conditions. The 2D streamlines show significantly stronger suction-side separation in the 38-blade configuration, indicating reduced flow guidance.

In contrast, the 44 blade configuration exhibits weaker separation. In both cases, separation due to low outlet pressure is present, while differences on the pressure side remain minor. However, the higher-blade-count case shows denser streamlines and a small recirculation region near the lower boundary.

At ADP and near surge, no significant differences are observed, as the flow fields and streamline patterns remain largely identical for both configurations. Overall, blade number reduction mainly affects separation behavior under choking conditions, while the global flow structures at ADP and near surge remain largely unchanged.

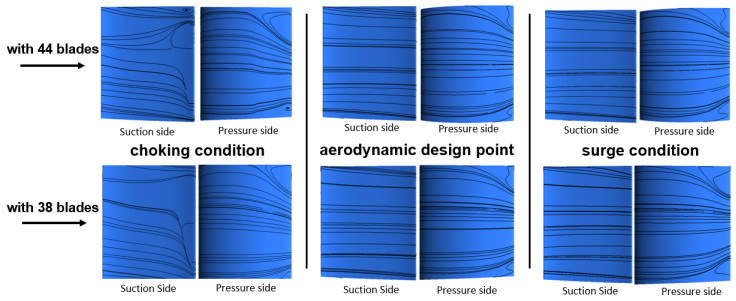

Figure 10: Streamlines over stator surface

3.2 Mass flow Density

Figure 11 shows regions of reduced axial mass flow density indicating local flow blockage within the stator passage. This blockage is primarily caused by boundary layer growth along blade surfaces and endwalls, as well as secondary flow structures such as passage vortices. As the boundary layer develops under adverse pressure gradients, the effective flow area decreases, forcing the core flow to redistribute.

This effect is more pronounced in the reduced solidity configuration, where higher blade loading intensifies diffusion and promotes earlier separation. Consequently, regions of low mass flow density are associated with low-momentum fluid, increased mixing, and higher total pressure losses, directly linking blockage to reduced aerodynamic efficiency [4].

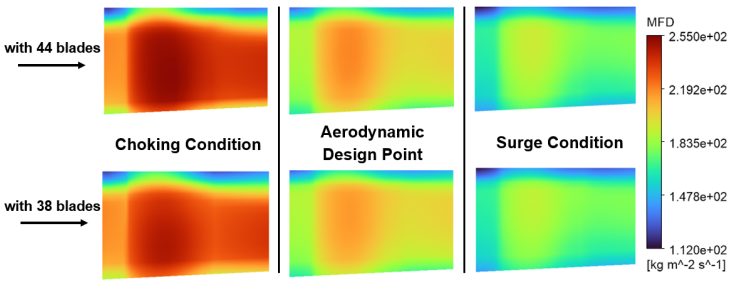

Figure 11: Mass flow density at stator outlet in a meridional view

3.3 Total pressure at stator outlet

At choking condition, the total pressure distribution at the stator outlet reveals the loss characteristics of both configurations. The 38 blade configuration shows a slightly more non-uniform distribution, with stronger low-pressure regions associated with wake development and increased mixing. In contrast, the reference configuration shows a more uniform total pressure field, indicating weaker wake structures and lower losses.

These differences are attributed to the reduced solidity in the 38-blade case, which increases blade loading and promotes boundary layer growth and separation. Consequently, the enhanced wake intensity leads to higher total pressure losses in the stator outlet flow.

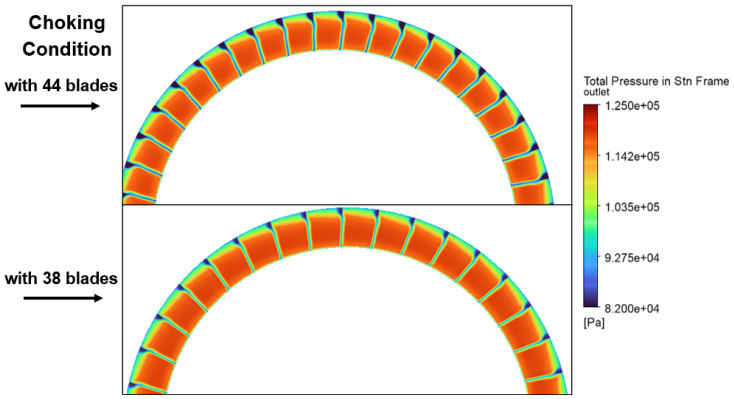

Figure 12: Total pressure at stator outlet at choking condition

Conclusion

The reduction in stator blade number from 44 to 38 maintains the overall compressor stage performance, as the rotor behavior remains essentially unchanged and the stage total pressure ratio is only marginally affected. The primary aerodynamic consequences are therefore confined to the stator flow field.

Within the stator, the reduced blade count increases the aerodynamic loading per blade and slightly reduces the flow turning capability. At the same time, the lower solidity raises the diffusion requirements within the passage, increasing sensitivity to adverse pressure

gradients and promoting boundary layer separation. These effects become particularly critical near the stability limit, where losses increase and the flow becomes more susceptible to separation.

Overall, the results demonstrate that blade number reduction introduces a clear trade-off between efficiency at high mass flow rates and aerodynamic robustness near surge, with the stator acting as the limiting component under off-design conditions.

References

[1] Oates, G. C., ed., *Aerothermodynamics of Aircraft Engine Components*, American Institute of Aeronautics and Astronautics, Inc., 1985.

[2] Gümmer, V., *Aerodynamic Design of Turbomachinery*, Chair of Turbomachinery and Flight Propulsion, Technical University of Munich, Garching, 2025.

[3] Gümmer, V., *Flight Propulsion 1 and Gas Turbines*, Vorlesung, Chair of Turbomachinery and Flight Propulsion, Technical University of Munich, Garching, 2025.

[4] Aungier, R. H., *Axial-Flow Compressors: A Strategy for Aerodynamic Design and Analysis*, ASME Press, New York, USA, 2003.

[5] Dixon, S. L., and Hall, C. A., *Fluid Mechanics and Thermodynamics of Turbomachinery*, 7th ed., Butterworth-Heinemann, Oxford, UK, 2014.